Experimental investigation of photovoltaic generator in alfresco condition

S. Bhattacharjee*, S. Bhakta, P.K. Mishra, T.K. Mouthik, R.K. Singh, S. Das, R. Kumar and M. Raj

Department of Electrical Engineering, National Institute of Technology (NIT), Agartala, India, Pin-799055
*** Corresponding author**: subhadeep_bhattacharjee@yahoo.co.in

ABSTRACT

Photovoltaic (PV) modules are used for generating electricity in PV power system. Solar light is converted directly into electricity with modules consisting of many PV solar cells. It is important to monitor the behaviour of PV modules under real field conditions to evaluate its tangible performance for a given site. The paper examines the PV module's performance for nine months of a year in an educational institute premise. Current-voltage and power-voltage characteristics, temperature dependence of the module, fill factor and efficiency analysis for different months have been explored. Normalised performance indices based on measured data have been investigated. Measured results have been compared with the estimated values by means of error statistics. It has been chronicled that peak solar power density reaches 971.04 W/m^2 while maximum PV power of 116 W/m^2 is produced during the characteristic day at noon. Working efficiency is achieved 9 – 11% during sun shine hours. Average monthly production factor is found to be 89.45%.

Keywords: *PV generator, solar irradiance, peak power, fill factor, efficiency, normalised parameters*

1. Introduction

Electricity generation using photovoltaic (PV) systems is important, reliable and has the potential to play a significant role in CO_2 emissions mitigation [1]. As a solution of depletion of conventional fossil fuel energy sources and serious environmental problems, focus on the PV system has been increasing around the world [2]. The most attractive features of solar panels are the nonexistence of movable parts, very slow degradation of the sealed solar cells, flexibility in the association of modules (from a few watts to megawatts), and the extreme simplicity of its use and maintenance [3]. Global PV electricity generating technology has sustained an impressive annual growth rate compared with other renewable energy generating technologies. It is widely accepted that PV will become one of the major future sources of electricity generation considering the declining cost of PV systems and expected achievement of grid-parity in many nations within few years [4, 5].

PV technologies are highly site specific and perform in a different way as regards to the environmental condition such as irradiance, temperature etc. The geographical location and all the linked meteorological variables can play a significant role on the energy outcome of a specific PV installation. Performance of PV modules is usually specified under standard test conditions (STC), but the response of the modules under real field conditions differs from the results under STC due to variety of continuously changing ambient parameters. For this reason, it is very much important to monitor and evaluate the performance of specific PV modules in their real working environment, and not relying solely on indoor tests and label data normally given under STC [6, 7]. As of January 2010, approximately 78% of the global installed capacity of solar PV power plants uses wafer-based crystalline silicon modules [8]. The paper analyses the performance of poly-crystalline silicon PV module in various times of the year. The investigation has been carried out during August'2012 to April'2013 in National Institute of Technology (NIT), Agartala which is located at one of the north-east (N-E) Indian states, Tripura. It is worth to be mentioned that Government of India (GoI) has taken special initiative to illuminate various remote areas of this part through solar electricity. Several cities of N-E India including Agartala have been declared as solar city by GoI to address energy challenges through a combination of enhancing supply from renewable energy sources in the city and energy efficiency measures [9]. But no experimental study has been carried out yet to examine the PV

generator performance in real field condition here. Hence, to monitoring the PV generator behaviour in outdoor operational environment is of paramount importance for successful dissemination of PV power system in this province. Results obtained from experimental investigations are compared with simulation based estimation through statistical analysis.

2. PV generator

2.1 PV generator modelling

Basically solar cell is a p-n junction semiconductor device that directly converts sun light into electricity through photovoltaic effect. The basic unit of PV generator (panel/array) is solar cell. The governing equations to explain the function of the PV generator are [10,11]:

$$I_{pv} = I_{ph} - I_o\left[\exp\left(\frac{V_{pv} + I_{pv}R_s}{V_t}\right) - 1\right] - \frac{V_{pv} + I_{pv}R_s}{R_p} \quad (1)$$

$$I_{ph} = I_{sc} + \frac{I_{sc}R_s}{R_p} \quad (2)$$

$$V_t = \frac{AkT_{STC}}{q} \quad (3)$$

$$V_{oc} = V_t In\left(\frac{I_{sc}}{I_o} + 1\right) \quad (4)$$

$$I_{sc} = \frac{G}{100}\left[I_{scr} + k_i\left(T_c - T_r\right)\right] \quad (5)$$

$$I_o = I_{or}\left(\frac{T_c}{T_r}\right)^3\left[e^{\frac{qE_g}{kA}\left(\frac{1}{T_r}+\frac{1}{T_c}\right)}\right] \quad (6)$$

$$T_c = \frac{T_{NOCT} - 20}{0.8}G + T_a \quad (7)$$

$$\eta = \frac{V_{pv}I_{pv}}{GA} \quad (8)$$

$$FF = \frac{P_{\max}}{V_{oc}I_{sc}} = \frac{V_{mp}I_{mp}}{V_{oc}I_{sc}} \quad (9)$$

Where I_{pv} is the generated current in the output of the PV cell, I_{ph} is the photo-generated current in STC, V_{pv} is the generated voltage in the output of the cell, I_o is the dark saturation current in STC, R_s and R_p are series and shunt resistances respectively, V_t is the junction thermal voltage, V_{oc} is the open circuit voltage, I_{sc} is the short circuit current, A is the diode quality (ideality) factor, k is the Boltzmann's constant (1.380×10^{-23} J/K), T_{STC} is the temperature at STC, q is the elementary charge constant (1.602×10^{-19} C), G is the insolation, T_c is the cell temperature, T_r is the reference temperature, I_{scr} is the short circuit current at the temperature T_r, k_i is the temperature coefficient of the short circuit current , I_{or} is the reverse saturation current at T_r, E_g is the band-gap energy of the

semiconductor, T_a is the ambient temperature , T_{NOCT} is the nominal operating cell temperature, η is the total efficiency of the PV cell, A is the area of the solar cell, FF is the fill factor (FF), P_{max} is the maximum power output, V_{oc} is the open circuit voltage, I_{sc} is the short circuit current, V_{mp} is the voltage at maximum power and I_{mp} is the current at maximum power.

2.2 Normalised performance parameters

To evaluate the performance of the PV generator, the PV system performance monitoring – guidelines for measurement, data exchange and analysis [12] and the International Energy Agency task II database on photovoltaic power system [13] are used. The system indices which are focused to assess the PV generator performance comprise: The array yield (Y_a), reference yield (Y_r), capture losses (L_c) and production factor (PF). These parameters are independent of the array size and are normalized by the array nominal installed power at STC, as given by the PV-module manufacturer in kW_p. These normalized parameters are expressed in terms of kWh/kW_p/day or hour/day (h/d).

The array yield is the daily array energy output (E_{dc}) per kW of installed PV array ($P_{pv,\ rated}$) and is given as:

$$Y_a = \frac{E_{dc}}{P_{pv,rated}} \tag{10}$$

The reference yield is the total daily in-plane solar irradiation H_t (kWh/m^2/day) divided by the array reference in-plane irradiance at STC (G_{ref}=1kW/m^2). Thus Y_r would be in effect, the number of peak sun-hours (PSH) per day and is given by:

$$Y_r = \frac{H_t}{G_{ref}} \tag{11}$$

Array capture losses are due to the PV array losses and are given as:

$$L_c = Y_r - Y_a \tag{12}$$

Production factor is determined as the energy produced per reference energy that the module should produce at STC. Thus it is expressed as:

$$PF = \frac{Y_a}{Y_r} \tag{13}$$

3. Experimental arrangement

3.1 PV module

The experimental set up shown in Figure 1 consists of two numbers of mono-crystalline modules and two numbers of poly-crystalline modules which are arranged diagonally. Each of these modules is 10 W_p rating. For experimental investigation in the present study, two series connected poly-crystalline modules are used. Table 1 gives the specifications of the modules at STC which have been used to test the performance of PV panel in open ambience.

Table 1 Module specifications

Material	Poly-crystalline silicon
Peak power output (P_{max})	10 W_p
Peak power voltage (V_{mp})	17 V
Peak power current (I_{mp})	0.59 A
Open circuit voltage (V_{oc})	21 V
Short circuit current (I_{sc})	0.6 A
Length	32.5 cm
Width	23 cm

Figure 1 PV module measuring set up

3.2 Measurement of solar irradiation

Though the global horizontal incidence (GHI) for a location at a given time can be estimated, it is better to measure the solar radiation wherever possible. In the present study, in the absence of pyranometer, a calibrated solar cell is used to measure the local solar radiation pattern. It is known fact that the current output of solar cells is a linear function of solar radiation. Also, the current output of solar cell does not depend strongly on the temperature of the solar cell .Consequently cell current can be used as a measure of solar irradiation at any point of time of daylight hours. The relationship is described as: Solar irradiation (W/m^2) = K × Cell current (A) where K is the proportionality constant. Normally solar cells in short circuit mode are used for measurement of solar irradiation.

The solar cell used in the present study (Figure 2) for irradiation measurement is a mono-crystalline silicon solar cell of 4 × 4 cm^2 area has been provided by National Centre for Photovoltaic Research and Education (NCPRE) of Indian Institute of Technology (IIT), Bombay during 1000 teachers training program of ministry of new and renewable energy (MNRE), Government of India.

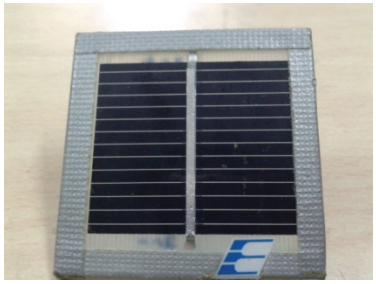

Figure 2 Calibrated solar cell

This solar cell has been calibrated against the pyranometer. The measured value of short circuit current and pyranometer readings is plotted in Figure 3. From the slope of the linear fit, the value of the K is obtained as 2175. It is specified with this solar cell that the accuracy of irradiation measurement is within 10% when solar radiation is more than 200 W/m^2 and within 25% when solar radiation is below 200 W/m^2.

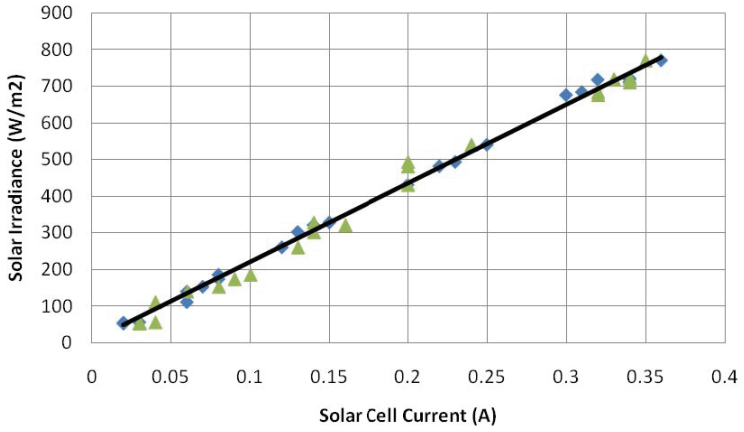

Figure 3 Measurement of solar cell current with measured value of solar irradiation using a pyranometer

4. Local climate data and site details

Table 2 presents the climatic information of the site where the experimental investigation has been carried out.

Table 2. Site details

Location	Agartala, India
Latitude	$23^0 52'$ N
Longitude	$92^0 50'$ E
Altitude	12.8m
Temperature	Maximum: 35^0C (summer), 28^0C (winter) Minimum: 20^0C (summer), 6^0C (winter)
Average wind velocity	2.86 m/s
Average rainfall per annum	363 cm

It is well known that the energy produced by a given PV system depends on several external factors. Foremost of these factors is of course the amount of solar irradiation impinging on the surface of the PV modules [14]. At any location on the earth surface, the solar radiation is a function of various atmospheric variables such as the extent of the cloud cover, the aerosol and the water vapour contents [15]. Thus the solar radiation can be direct, diffused or reflected radiation. Using the 22 years averaged data from the NASA's (National Aeronautics and Space Administration, USA) surface solar energy data set [16], diffused to global and direct to global solar radiation pattern of the site is plotted in Figure 4. It reveals the annual trend of percentage variation of direct and diffused solar fraction which is found to be complementary in nature. It is observed that during winter (i.e. November – February), ratios of diffused to global solar radiation are high as regards to summer (April – May) and rainy periods (June – August). Accordingly, at the same time percentage of direct radiation contributing to global radiation is low. Nevertheless, in any case, diffused fraction does not exceed 50% in any phase of the year.

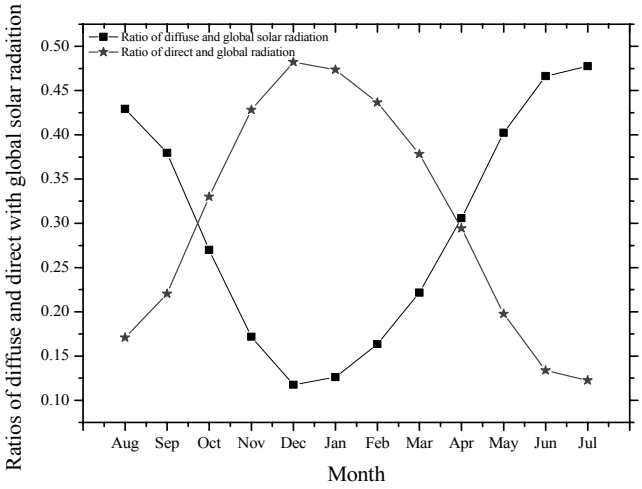

Figure 4 Amount of direct and diffused component in total in-plane solar insolation

5. Results and discussions

5.1 Solar insolation and temperature

Figure 5 shows the measured monthly averaged total in-plane insolation together with the monthly ambient temperature averaged over the daytime hours. The highest value of total in-plane insolation is in March with 0.46 kW/m^2 and the lowest in September is 0.34 kW/m^2. The observed temperature ranges from 21 ^{o}C (December) to 34 ^{o}C (April) with mean ambient temperature of 29.74 ^{o}C.

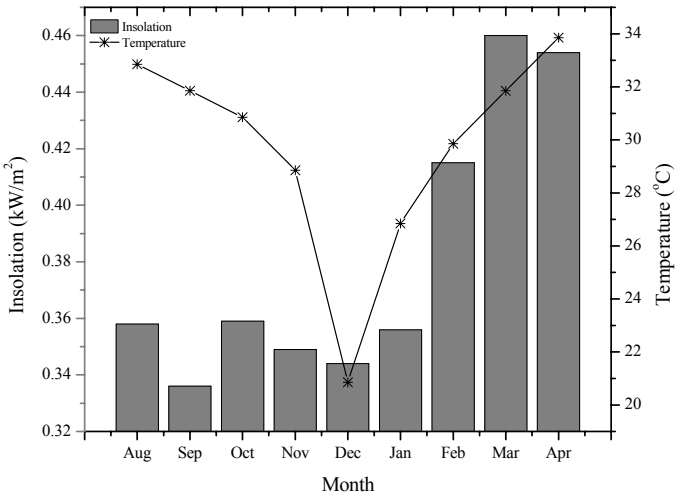

Figure 5 Monthly averaged total in-plane solar insolation and mean ambient temperature variation

Figure 6 shows the measured global irradiance pattern of four consecutive days for the month February. It is observed that on 9th February the irradiance is lesser compared to next three consecutive days due to the effect of variables like sun hours, air temperature, relative humidity, shading effects, cloudiness etc. The highest irradiance is recorded in 10th February which suggests better clear sky global radiation on this particular day compared to other nearby days. Drastic changeability in irradiance pattern is observed on 11th February, possibly due to the result of the variation of atmospheric circulation in the site. It is perceived from the measured solar radiation sample that successive days correlate well and solar radiation is stable in general in the site. Peak solar radiation is found to be varied from 600 – 1000 W/m^2 during these four consecutive days.

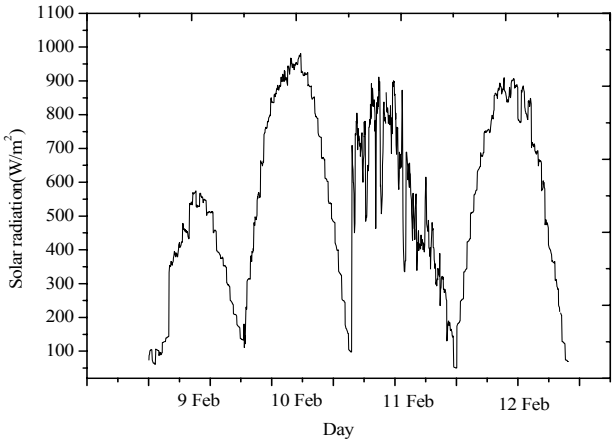

Figure 6 Solar radiation sample for few consecutive days

5.2 Current-voltage and power-voltage characteristics

Figure 7 shows the Current-voltage (I-V) and power-voltage (P-V) characteristics of the 20 W_p module for twelve months of the year and also in STC. The results are obtained in simulation with Matlab considering the average solar radiation values of NASA's surface solar energy data set.

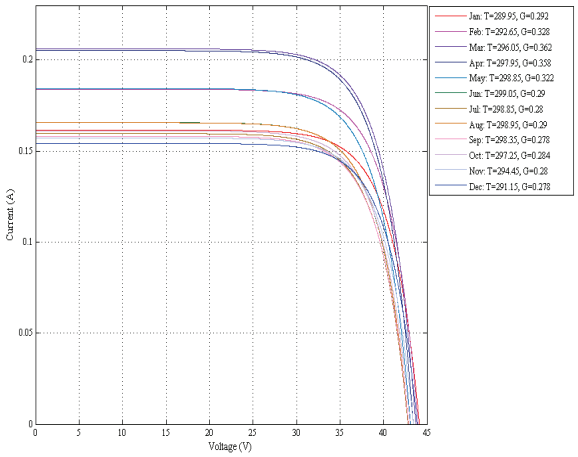

Annual I-V curves of the module

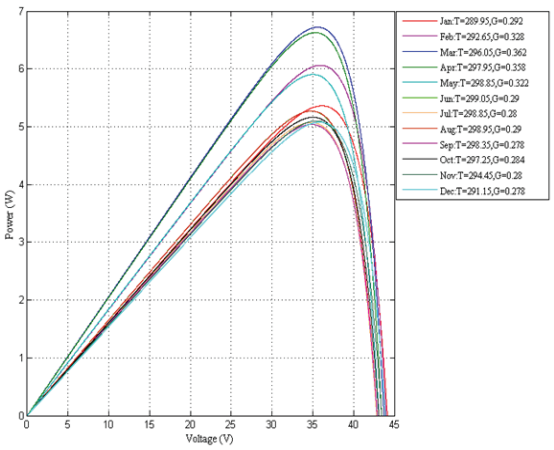

Annual P-V curves of the module

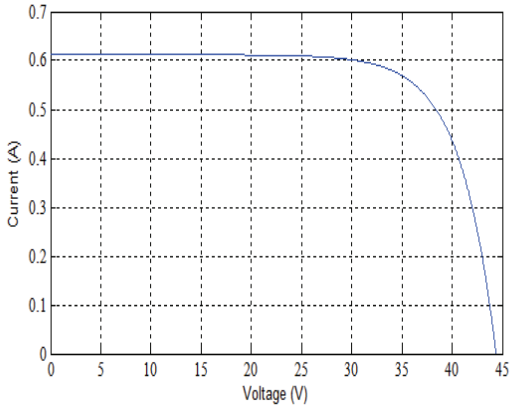

I-V characteristic of the module at STC

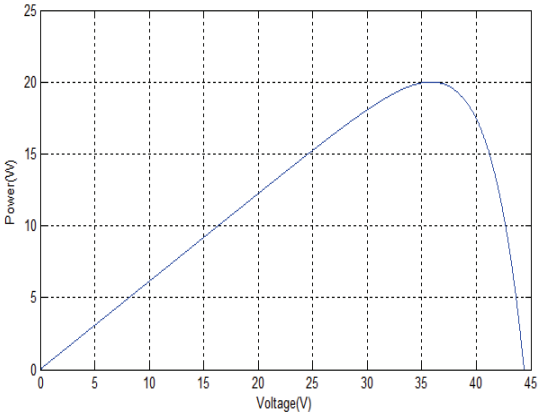

P-V characteristic of the module at STC

Figure 7 I-V and P-V characteristics of 20 W_p module in simulation

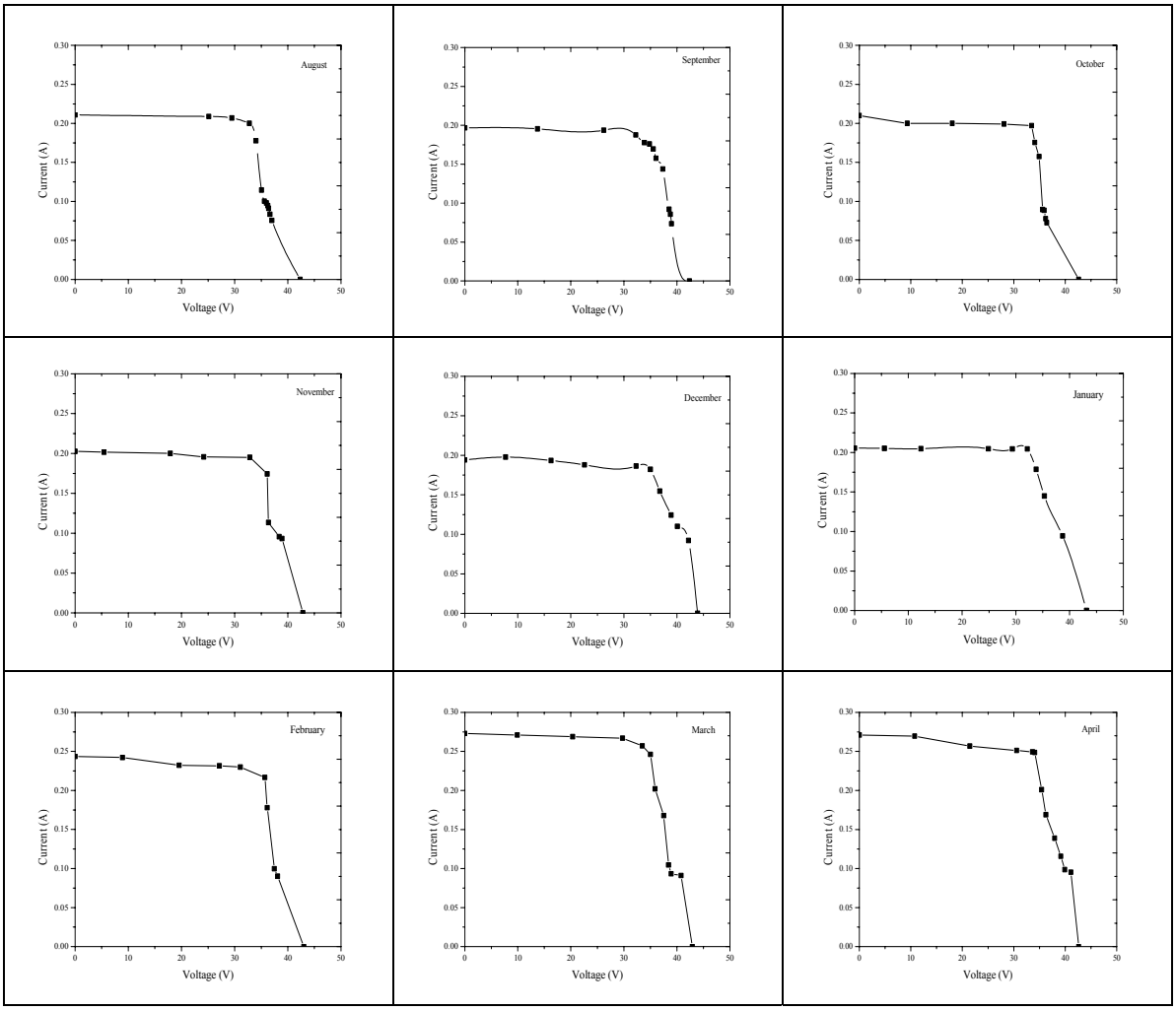

Figure 8 Measured I-V characteristics of the 20 W_p module in various months of the year

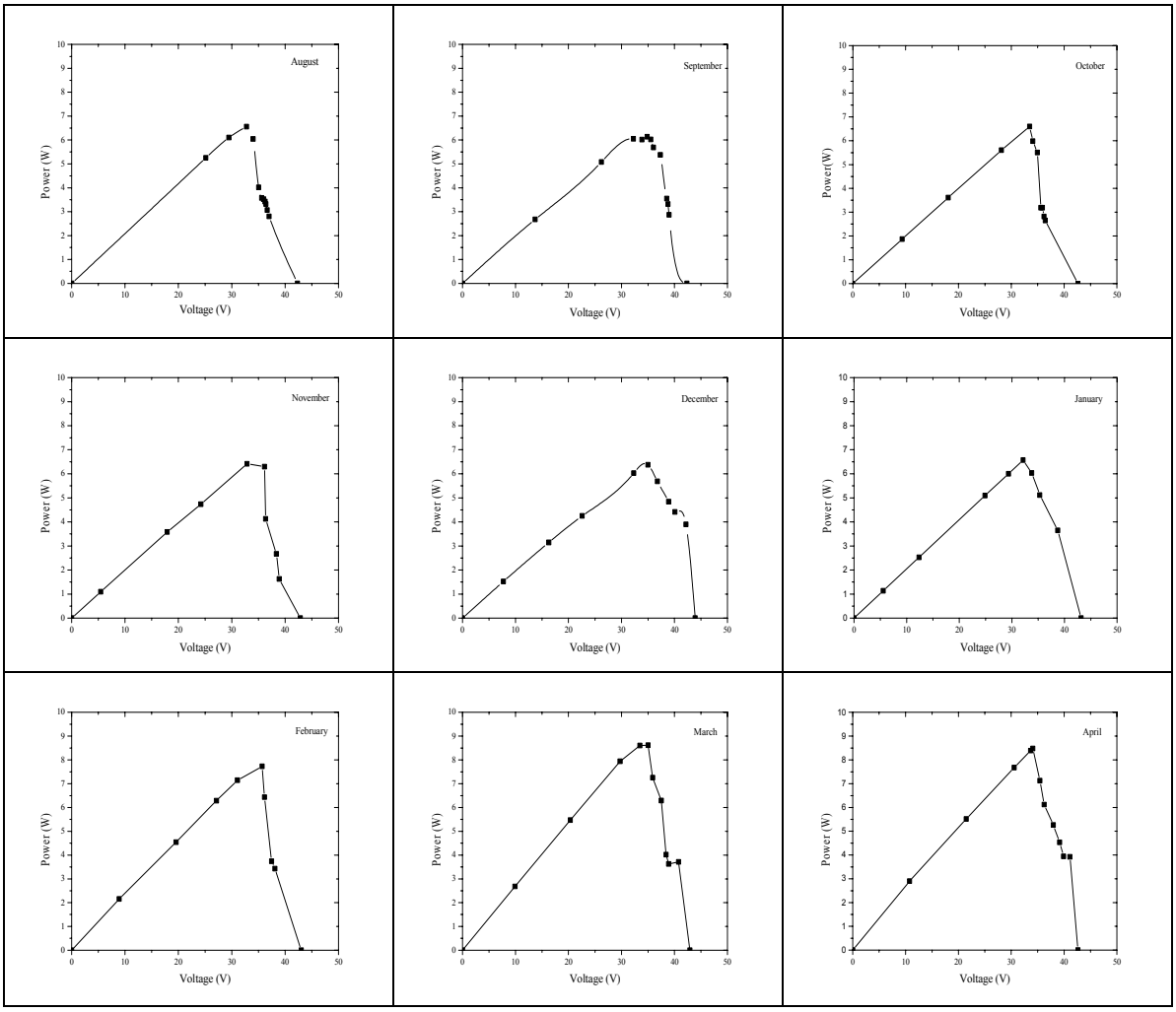

Figure 9 Measured P-V characteristics of the 20 W_p module in various months of the year

Figure 8 and Figure 9 plot the measured I-V and P-V characteristics of 20 W_p module in various months of the year. In order to find out various current-voltage points of PV module, resistance of different values must be connected with the module. In this work, a rheostat (0-200 Ω, 2.5 A) has been used to obtain various operating points. The operating point of the solar cell depends on the magnitude of the load resistance, which is the output voltage divided by the load current. The intersection of the PV module characteristics with the load line is the operating point of the PV module. It is observed from Figure 8 that open circuit voltage stays almost constant (42 – 43 V) whereas short circuit current ranges from 0.19 A to 0.27 A. Simulation results shown in Figure 7 also indicate that open circuit voltage is in the order of 43 to 44 V and short circuit current varies between 0.16 A and 0.22 A as compared to open circuit voltage of 42 V and short circuit current of 0.6 A at STC. Figure 9 shows the measured maximum values of power lie between 6.5 W and 8.5 W whereas simulation results (Figure 7) range between 5 W and 7.7 W.

5.3 Temperature dependence of open circuit voltage

The open circuit voltage as a function of temperature is found by linear regression. The data presented in Figure 10 reveals that an increase in the temperature decreases the open circuit voltage of the PV module. It is hard to investigate the dependence of only the temperature on open circuit voltage when the PV module is installed in an open environment. In a natural environment, all localized climatic parameters act concurrently on the module and its response represents the combined effect of these parameters on the performance of the module.

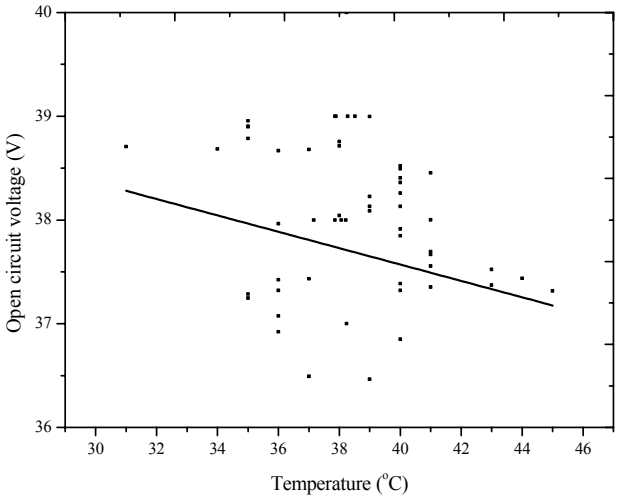

Figure 10 Measured open circuit voltage versus temperature

5.4 PV power output

The daily power profile of PV module and solar radiation for a characteristic day (10th February'2013) is shown in Figure 11. The solar power density (global irradiance) during a typical day with stable weather follows the bell-shaped curve. The output power of the module is also a bell shaped curve. It is observed that 80 – 115 W/m^2 solar electricity is produced for approximately 5 hours for a typical day against solar power density of 750 – 1000 W/m^2. Peak solar power density reaches 971.04 W/m^2 and maximum PV power of 116 W/m^2 is produced during the day at 12:01 pm. Figure 12 shows the power output of the module versus the measured solar power density. The output power of the PV module is linearly related to solar power density. It is clear that as the intensity of solar irradiance incident is more, more will be the power produced.

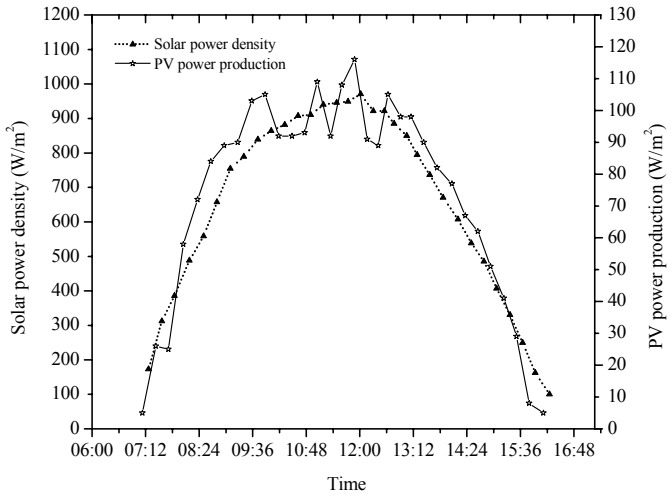

Figure 11 Electricity production and solar power density in a characteristic day

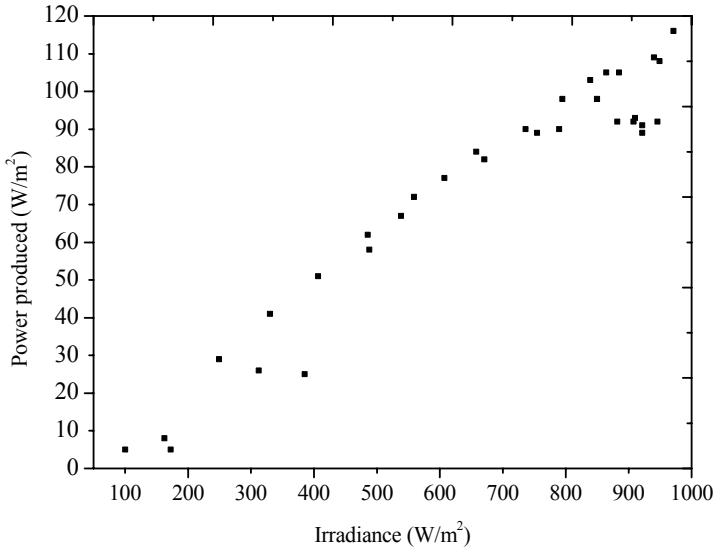

Figure 12 Produced power per square meter versus global irradiance

Figure 13 depicts the average monthly peak power profile of the module under test. Variations of peak power in different months occur due to the variability of solar irradiance, temperature, array capture losses, etc. Both estimated and measured results indicate that maximum peak power is obtained in March and minimum peak power is found to be in September. This is possibly because of the total in-plane solar radiation that attains the highest and the lowest in March and September respectively.

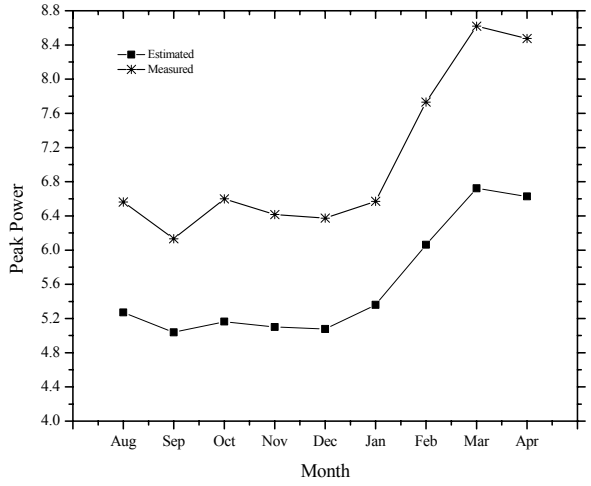

Figure 13 PV module peak power variation in different months

5.5 Fill factor

Fill factor is the ratio of the maximum power of the PV device to the product of open circuit voltage and short circuit current. Fill factor is an indication of maximum utilization of the array size for the generation of the maximum power. The working temperature which influences the changes in the maximum power also influences the changes in fill factor. With increase in temperature, open circuit voltage of the PV module decreases with slight increase in short circuit current. But the temperature changes have little effect on short circuit current but affect the open circuit voltage considerably. Thus the fill factor is reduced as the temperature of the device is increased. Figure 14 represents the estimated and measured values of fill factors for different months of the year. In the winter months (December – February), higher values of fill factors are observed as the ambient temperature remains

low during that time. Measured values of the fill factors in field conditions are ranged between 0.73 and 0.75.

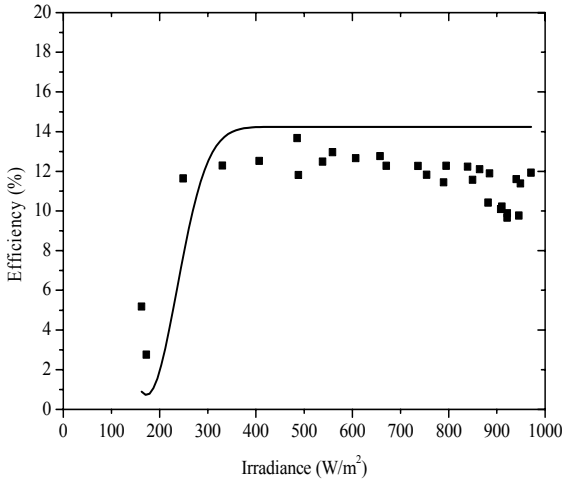

Figure 14 Averaged monthly fill factor of the PV module

5.6 Efficiency analysis

The efficiency of the PV module against irradiance is plotted in Figure 15 for a characteristic day. Low efficiencies of 2.75% and 5.18% are chronicled corresponding to low irradiance intensities of 172.81 W/m^2 at 7:16 am and 100.45 W/m^2 at 4:15 pm respectively. With gradual increase in irradiance, the efficiency has shown a steep rise till the start of the peak functioning period. It is observed that the constant working efficiency of 9-11% is achieved by the system. The graphical representation of the efficiency versus irradiance is approached with the Gaussian regression approximation to assess the level of constancy in the working efficiency of the PV module in normal conditions.

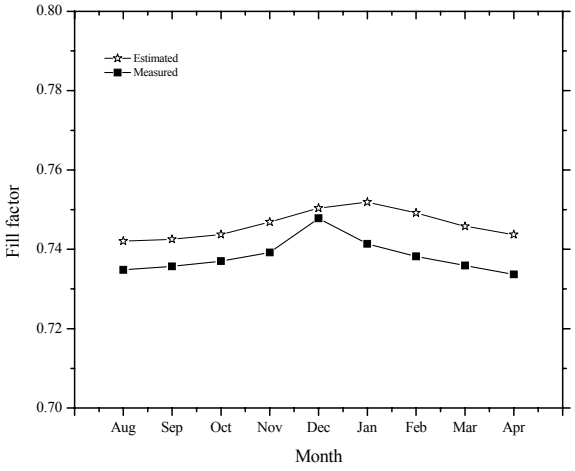

Figure 15 Module efficiency versus measured global irradiance

The daily distribution of the module efficiency for a characteristic day is shown in Figure 16. The PV system efficiency remains almost constant at around 10 – 12% during most of the hours of the daylight. Lower efficiency is recorded in the early morning and in the late afternoon. 3% is observed in the morning around 7:12 am and 5.18% in the late afternoon around 4:15 pm. In the early morning and late afternoon, the solar irradiance levels are much lower and some cells do not even receive the

minimum solar energy for electricity generation. Due to this partial operation of the solar cells, efficiency values are obtained around 3-5% in morning and late afternoon.

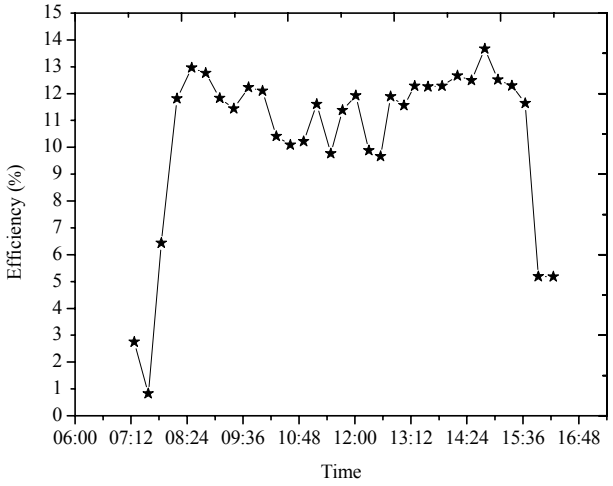

Figure 16 Efficiency in a characteristic day

Figure 17 depicts the estimated and measured values of efficiency for different months. Measured value of efficiency ranges between 4.10% (September) and 5.76% (March) whereas estimated range of efficiency is found to be 3.37% (September) to 4.50% (March). It is perceived that measured results strongly observe the estimated one.

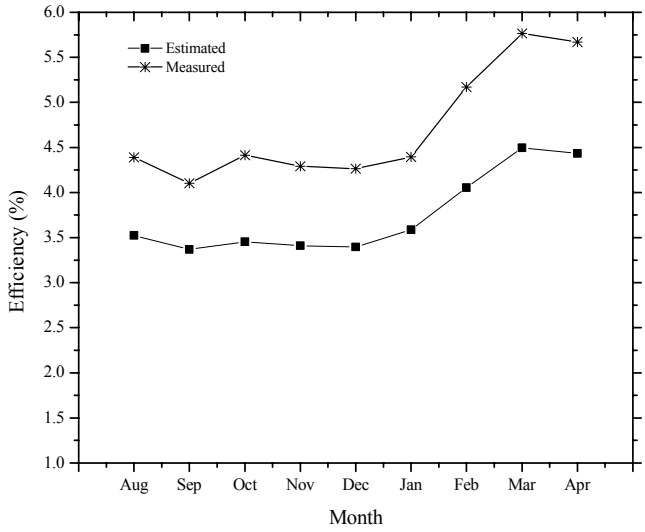

Figure 17 Monthly distribution of the efficiency

5.7 Normalised performance parameters

Electrical performance of the PV generator in terms of normalised representation of energy and power is depicted in Figure 18. These indicators are related to the incident energy in the collector plane, and are normalised by the array nominal installed power at STC, as given by the PV-module manufacturer in kW_p. Therefore, they are independent of the array size, the geographic situation and the field orientation. Figure 18 shows the monthly average daily PV system's array yield, array capture losses, and production factor during the nine months of the monitoring period. Both estimated and measured

values of normalized performance parameters are evaluated in the figure. Measured array yield varies from 3.68 kWh/kW$_p$/day (September) to 5.17 kWh/kW$_p$/day (March) with average value of 4.23 kWh/kW$_p$/day whereas estimated values ranges from 3.02 kWh/kW$_p$/day (September) to 4.03 kWh/kW$_p$/day (March) with mean value of 3.36 kWh/kW$_p$/day. The range of measured and estimated capture losses are observed to be 1.50 kWh/kW$_p$/day (December) to 1.83 kWh/kW$_p$/day (March) and 1.24 kWh/kW$_p$/day (November) to 1.55 kWh/kW$_p$/day (April) with mean values of 1.65 kWh/kW$_p$/day and 1.36 kWh/kW$_p$/day respectively. The measured and estimated production factors are ranged individually from 85.19% (September) to 92.84% (March) and from 69.96% (September) to 72.40% (March) over the monitoring period.

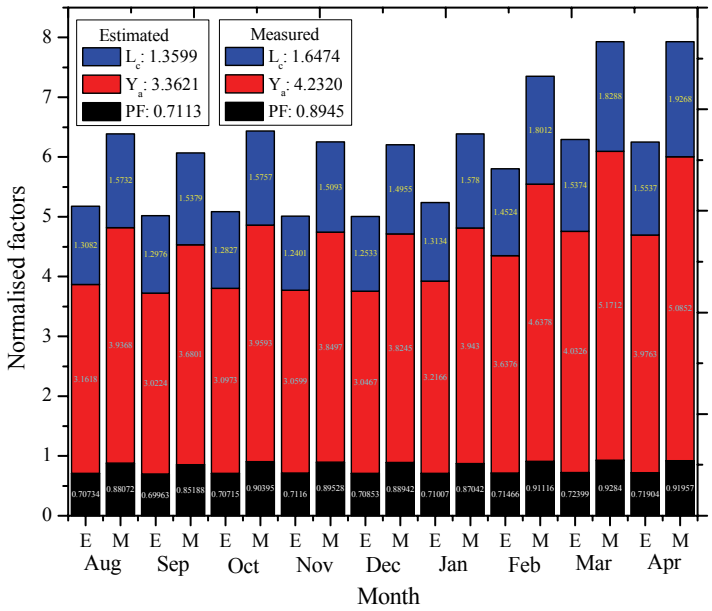

Figure 18 Monthly averaged daily array yield, array capture losses and production factor

6. Statistical analysis of measured and estimated results

The experimentally determined performance analysis results in outdoor condition are compared with estimated values for validation of measurement. Environmental factors such as irradiance and temperature data have been used from twenty two years averaged satellite data of NASA's surface solar energy data set to estimate the PV module's electrical parameters. The comparison is evaluated through statistical analysis using mean bias error (MBE), root mean square error (RMSE), and correlation coefficient (r). It is desirable to have the lowest possible values for MBE, RMSE and highest possible values for r [17]. Table 3 illuminates the amount of deviation or closeness between the measured and the estimated values. Statistical examination between indirect satellite data and in situ measured data of irradiance are also incorporated in Table 3. MBE reveals whether a given analysis has a tendency to under- or over-predict, with the MBE values closer to zero being desirable. RMSE presents a measure of the variation of two sets of values. Lower RMSE values are, the better the results are in terms of its absolute deviation. The correlation coefficient gives an indication on how much the two data are close to each other. The high value of correlation coefficient indicates that there is a good linear relationship between indirect and estimated results. Hence, results shown in Table 3 are self explanatory. In most of the cases values are close enough to comprehend that measurement based results are reasonable.

Table 3. Error statistics between measured and estimated results.

PV module's parameter	Outcome of statistical examination		
	MBE	RMSE	r
Irradiance	-0.0757	0.0049	0.9955
Temperature	-7.6944	2.4449	0.8154
Array yield	-0.8700	0.0610	0.9950
Capture loss	-0.2875	0.0306	0.9838
Production factor	-0.1832	0.0036	0.8850
Open circuit voltage	0.7478	0.4042	0.6170
Short circuit current	-0.0513	0.0030	0.9958
Peak Power	-1.4512	0.1019	0.9950
Efficiency	-0.9707	0.0682	0.9950
Fill factor	-0.0081	0.0028	0.7911

7. Conclusion

PV electricity generation technique has been increasingly adopted across the world in recent years due to energy security and environmental reasons. The technology has become popular in many parts of the world. The present paper experimentally explores the behavior of PV generator in real outdoor environment. Most of the analyses with field measurement during the monitoring period of nine months have been compared with that of estimated one. Comparison through error statistics indicates that measured results are by and large good to be accepted. Moreover, better measured values have been obtained than the predicted one which directs towards the improved performance of PV modules at actual situation. It is observed that in-plane solar insolation varies within 0.34 – 0.46 kW/m^2 at the investigation site. Open circuit voltage and short circuit current are found to be 42 – 43 V and 0.19 – 0.27 A respectively whereas peak power is recorded in the range of 6.5 – 8.5 W during observation period. It is chronicled that in a characteristic day, 80 – 115 W/m^2 solar electricity is produced for approximately 5 hours duration. During most of the sunlight period, 9 – 11% efficiency is achieved from PV generator in a typical day. Fill factor ranges from 0.73 to 0.75. Average normalised performance indices based on measurement are found as 4.23 h/d, 1.65 h/d, and 89.45% for array yield, capture losses, and production factor respectively.

Acknowledgement

Authors acknowledge the contributions of National Centre for Photovoltaic Research and Education (NCPRE) of Indian Institute of Technology (IIT), Bombay for providing the experimental arrangements during 1000 teachers program on photovoltaic fundamentals, technologies and applications, supported by Ministry of New and Renewable Energy of Government of India.

Reference

[1] Nawaz, I., and Tiwari, G.N., 2006. Embodied energy analysis of photovoltaic (PV) system based on macro- and micro-level. *Energy Policy*, 34, 3144 – 3152.

[2] So, J.H., Jung, Y.S., Yu, G.J., Choi, J.Y., and Choi, J.H., 2007. Performance results and analysis of 3 kW grid-connected PV systems. *Renewable Energy*, 32, 1858 – 1872.

[3] Farret, F.A. and Simões, M.G. (2006). *Integration of alternative sources of energy.* New Jersey, USA: John Wiley and Sons, Inc.

[4] Bhandari, R., and Stadler, I., 2009. Grid parity analysis of solar photovoltaic systems in Germany using experience curves. *Solar Energy*, 83, 1634 – 1644.

[5] Ayompe, L., Duffy, A., McComack, S., Conlon, M., 2010. Measured performance of a 1.72 kW rooftop grid connected photovoltaic system in Ireland. *Energy Conversion and Management*, 52, 816-825.

[6] Kurnik, J., Jankovec, M., Brecl, K., and Topic, M., 2011. Outdoor testing of PV module temperature and performance under different mounting and operational conditions. *Solar Energy Materials and Solar Cells,* 95, 373 – 376.

[7] Colli, A., and Zaaiman, W.J., 2012. Maximum-power-based PV performance validation method: application to single-axis tracking and fixed-tilt c-Si system in the Italian alpine region. *IEEE Journal of Photovoltaics*, 2, 555 – 563.

[8] Miller, A., and Lumby, B. (2012). *Utility scale solar power plants – A guide for developers and investors*. New Delhi, India: International Finance Corporation (IFC), World Bank Group.

[9] http://www.mnre.gov.in/schemes/decentralized-systems/solar-cities/ (accessed on June 6th, 2013).

[10] Kymakis, E., Kalykakis, S., and Papazoglou, T.M., 2009. Performance analysis of a grid connected photovoltaic park on the island of Crete. *Energy Conversion and Management*, 50, 433 – 438.

[11] Castañeda, M., Cano, A., Jurado, F., Sánchez, H., and Fernández, L.M., 2013. Sizing optimization, dynamic modeling and energy management strategies of a stand-alone PV/hydrogen/battery-based hybrid system. *International Journal of Hydrogen Energy*, 38, 3830 – 3845.

[12] Photovoltaic system performance monitoring – guidelines for measurement, data exchange and analysis, IEC standard 61724, 1998.

[13] Jahn, U., Mayer, D., Heidenreich, M., Dahl, R., Castello, S., Clavadetscher, L., Frölich, A., Grimmig, B., Nasse, W., Sakuta, K., Sugiura, T., Borg, N., and Otterdijk, K., International Energy Agency PVPS Task 2: Analysis of the operational performance of the IEA database PV systems. *16th European Photovoltaic Solar Energy Conference and Exhibition*, May 2000, Glasgow, UK.

[14] Huld,T., Gabi F., Skoczek, A., Kenny, R.P., Sample,T., Field, M., and Dunlop, E.D., 2011. A power rating model for crystalline silicon PV modules. *Solar Energy Materials & Solar Cells*, 95, 3359 – 3369.

[15] El Shazly, S.M., Hassan, A.A., Kassem, K.O., Adam, M.E., and Ahmed, Z.M., 2011. Estimating global and diffuse solar radiation from sunshine duration at Qena/Egypt, *Canadian Journal on Computing in Mathematics, Natural Sciences, Engineering and Medicine*, 2, 237 – 261.

[16] Surface meteorology and solar Energy: A renewable energy resource web site (release 6.0). (https://eosweb.larc.nasa.gov/sse/).

[17] Sonmete, M.H., Ertekin, C., Menges, H.O., Haciseferoğullari, H., and Evrendilek, F., 2011. Assessing monthly average solar radiation models: a comparative case study in Turkey. *Environmental Monitoring and Assessment*, 175, 251 – 277.